

Article

Autonomous Soil Water Content Sensors Based on Bipolar Transistors Encapsulated in Porous Ceramic Blocks

Pedro Carvalhaes-Dias^{1,2,3}, Flávio J.O. Morais⁴, Luís F. C. Duarte^{1,3} , Andreu Cabot^{2,5}
and J. A. Siqueira Dias^{2,3,*} 

¹ Paraná Federal University of Technology—UTFPR, Cornélio Procópio PR 86300-000, Brazil; pcdias@utfpr.edu.br (P.C.-D.); lfduarte@utfpr.edu.br (L.F.C.D.)

² Catalonia Institute for Energy Research (IREC), Jardins de les Dones de Negre 1, 08930 Barcelona, Spain; acabot@irec.cat

³ Department of Semiconductors, Instruments and Photonics, School of Electrical and Computer Engineering, University of Campinas, Campinas SP 13083-820, Brazil

⁴ Faculty of Science and Engineering, São Paulo State University Júlio de Mesquita, Tupã SP 17602-496, Brazil; fjom@tupa.unesp.br

⁵ Institució Catalana de Recerca i Estudis Avançats (ICREA), Pg. Lluís Companys 23, 08010 Barcelona, Spain

* Correspondence: siqueira@demic.fee.unicamp.br; Tel.: +55-19-3521-4901

Received: 16 February 2019; Accepted: 11 March 2019; Published: 22 March 2019



Abstract: We present an autonomous sensor to measure soil water content that uses a single heat pulse probe based on a transistor encapsulated in a porous block. The sensor uses a bipolar junction transistor, which performs as both a heating and temperature-sensing element. Since the sensor depends on a porous block to measure the matric potential of the soil, it does not suffer from accuracy problems if the contact between the probe and the soil is not perfect. A prototype of the sensor showed a temperature variation of $\Delta T = 2.9^\circ\text{C}$ when the porous ceramic was saturated with water. The sensor presented an almost linear behavior for small changes in the matric potential of a red latosol when tested in the 1-kPa and 35-kPa pressure range, showing a sensitivity of $S = 0.015^\circ\text{C}/\text{kPa}$. The ultra-low power signal conditioning circuit can read the sensor's temperature with a resolution of approximately 0.02°C , so the matric potential can be read in increments of at least 1.33 kPa. When powered only by a 2-F supercapacitor from the energy-harvesting system, the interrogation circuit is able to take one soil water content measurement per day, for eleven days.

Keywords: soil water content; porous ceramic; bipolar transistor; embedded circuits; heat dissipation soil moisture sensors; low-power circuits

1. Introduction

Due to space variability [1], precision agriculture and advanced irrigation management systems require the use of a large number of reliable and accurate soil water content sensors [2]. Although many types of soil water content sensors have been developed (time-domain reflectometry [3], tensiometers, electrical resistance blocks, electromagnetic conductivity meters [4]), one of the most used low-cost soil water content sensors are the heat pulse probe sensors. The various types of heat pulse probes (button heat pulse probes (BHPP) [5,6], dual heat pulse probes (DHPP) [7], and single heat pulse probes (SHPP) [8]) operate based on heat capacity measurements.

The SHPP sensors (discussed in this work) have a heating element and a temperature-sensing device inserted inside a metal cylinder filled with thermally-conductive epoxy, which is put in direct contact with the soil. A heat pulse is applied to the heating element for a fixed period of time (typically

in the range of 10–30 s), and at the end of the pulse, the temperature rise is measured using the temperature-sensing element.

The temperature rise in the probe inserted into the soil depends on the thermal conductivity of the material that surrounds the sensor. Since the heat capacity of the soil depends on its water content, the temperature rise measured in the sensing element can be related to the soil water content [9].

However, if the contact between the probe and the soil is not perfect, the soil water content measurement results can be very inaccurate, and a very efficient solution to this weakness is to manufacture the SHPP sensors encapsulating the heating element and the temperature sensor within a porous block [10,11].

The operation of porous block soil water matric potential sensors depends on the characteristics of the porous material. When a sensor with a porous block is inserted into the soil, the water flows between the porous ceramic and the soil until an equilibrium is reached, even if the the sensor's contact with the soil is not good. By measuring the thermal conductivity of the porous ceramic filled with water, accurate estimations of the water content in the soil surrounding the sensor can be obtained. The use of a porous ceramic block is so efficient in overcoming the soil contact problems that even capacitive sensors have been fabricated using porous blocks [12].

Recently, we presented a novel technique for the fabrication of SHPP sensors, where the metal cylinder with the heating element (resistor) and the temperature-sensing element (thermistor or thermocouple) were replaced by a single bipolar transistor, which acts both as the heating and temperature-sensing element [13]. Although there are many advantages in using such a sensor, because it is very low cost and the fabrication is extremely simple (the sensor is actually a commercial transistor), it suffers from the soil contact problem.

In this work, we present a highly improved version of the single transistor soil water content sensor, obtained by encapsulating the transistor in a porous ceramic block (to mitigate the problems originated from the uneven contact of the sensor's surface with the soil). We also designed a new signal conditioning circuit, providing the possibility of autonomous operation of the system when powered by an energy-harvesting system (such as those presented in [14]), by using a low-power heat pulse and an ultra-low-power signal conditioning circuit.

2. Principle of Operation of the Single Transistor Soil Water Content Sensor

The bipolar transistor in this soil water content sensor has to perform as both the heating and temperature-sensing element. The transistor is heated with a fixed power pulse, obtained by applying a current pulse with a fixed collector voltage and with a duration $\Delta t = t_f - t_0$. During the operation of the sensor, the values of the transistor's V_{BE} are measured using an analogue-to-digital converter (A/D) embedded in the microcontroller that controls the measurement procedure and calculates the soil water content. The values of V_{BE} are used to calculate the sensor's temperature.

A diagram of the measurement scheme and a typical curve of the temperature rise and the V_{BE} as a function of the time, for an SHPP sensor, is shown in Figure 1.

The variation of V_{BE} with temperature is well known [15]. For a transistor biased with a constant collector current I_{C0} , it can be conveniently expressed as the sum of a constant term, a linear term (which decreases with temperature), and a term that is non-linear with temperature [16]:

$$V_{BE}(T) = \left(V_{g0} + \eta \frac{kT_r}{q} \right) - \lambda T + \eta \frac{k}{q} \left[T - T_r - T \ln \left(\frac{T}{T_r} \right) \right] \quad (1)$$

where:

$$\lambda = \frac{\left(V_{g0} + \eta \frac{kT_r}{q} \right) - V_{BE}(T_r)}{T_r} \quad (2)$$

and V_{g0} is the extrapolated band-gap voltage at 0 K; η is a constant (dependent on the transistor fabrication process), and T_r is a reference temperature, in K.

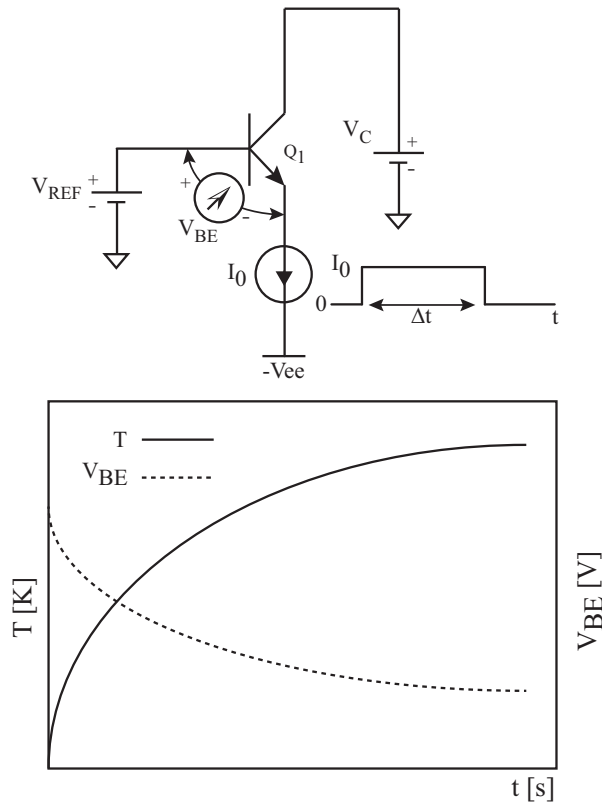


Figure 1. Basic measurement scheme of a single transistor soil water content sensor and a typical measured curve of the temperature rise as a function of time.

Thus, by measuring the V_{BE} of a transistor biased with a constant current I_{C0} at a known temperature T_r , it is possible to calculate the value of λ for the transistor when it is biased with I_{C0} . With the value of λ calculated, it is possible to calculate the temperature T of the transistor by measuring the value of its V_{BE} .

Since the value of λ is in the order of ≈ 1.8 mV/K and the last term of Equation (1) (a non-linear term) is typically in the order of $10 \mu\text{V/K}$, $V_{BE}(T)$ is usually approximated by the constant and linear terms of Equation (1):

$$V_{BE}(T) = \left(V_{g0} + \eta \frac{kT_r}{q} \right) - \lambda T \tag{3}$$

and this approximation is used to calculate the temperature of the sensors in this work.

Before the transistor is encapsulated in the porous ceramic block (from Hidrosense Ltda), the value of V_{BE} of the transistor is measured, at a known temperature T_r , in two situations: with $I_C = 100 \mu\text{A}$, and $I_C = 10$ mA. These measured values of V_{BE} are used to calculate the values of the λ of the transistors in these two situations, so that we can easily calculate the temperature of the sensor before the application of the heat pulse (with $I_C = 100 \mu\text{A}$) and during the application of the heat pulse (with $I_C = 10$ mA), by simply measuring the values of V_{BE} during these measurement phases.

The initial value of the sensor's temperature (before the heat pulse is applied) is obtained with the transistor biased with $I_C = 100 \mu\text{A}$. With this value of V_{BE} , we can precisely calculate the value of the sensor's temperature, which is in thermal equilibrium with the soil. The sensor's response depends on the soil's temperature, so the calibration must be performed at different soil temperatures. For each calibration temperature, the value of V_{BE} (the soil's temperature) must be written, and a table with the results of calibration and its associated soil temperatures must be stored in the microcontroller.

If a heat pulse of duration of $\Delta t = t_f - t_0$ is applied to a SHPP sensor, reference [9] showed that the temperature change $\Delta T = T_f - T_0$ can be approximated by:

$$\Delta T = T_f - T_0 = \frac{Q_l}{4\pi k_s} \ln(t_f - t_0) \quad (4)$$

where T_0 and T_f are the initial and final temperature, measured at times t_f and t_0 , Q_l is the heat input per unity length of the heater (W/m), and k_s is the thermal conductivity of the soil (W/mK). Therefore, by measuring ΔT as a function of time, we can calculate k_s and correlate its value with the soil water content.

The initial transient of temperature that occurs immediately after the heat pulse is applied is usually discarded, and the temperature is measured only after t_0 , which is taken at 1 or 2 s after the instant that the heat pulse is applied.

It is important to notice that, although the soil's thermal conductivity depends on its water content, the thermal conductivity is also affected by both the soil's contents of mineral and organic material and its density [17,18], and before using the sensor in a soil, an experimental calibration procedure in the laboratory is required. In the field, the sensors are used at a maximum rate of one reading per day, but usually only one reading is taken every three or four days.

3. Signal Conditioning Circuit

3.1. Power Management Circuits

The signal conditioning system presented in [13] is a complex laboratory equipment that uses relatively high voltages (+25 V and −5 V) to work and is not adequate to be integrated in an autonomous irrigation management system powered by energy harvesters [19].

In this work we present a signal conditioning system that operates from a single 5-V power supply, obtained from an energy-harvesting system with a supercapacitor, based on a DC microgenerator attached to the top of an irrigation micro-sprinkler [12]. The simplified block diagram of the developed power management circuit is presented in Figure 2.

The main supply voltage is taken from an "ORed" connection of the voltages derived from: (a) a supercapacitor (which is charged up to 5.2 V); (b) the voltage at the output pin V_{out} of IC_5 , an LTC3108 DC-DC converter from Analog Devices, which can reach 5 V when the steady state of the LTC3108 is reached. The voltage taken from the supercapacitor V_{Cstore} has two series Schottky diodes D_3, D_4 (BAT43 from STMicroelectronics), while the V_{out} has only one BAT43 diode (D_5) in series.

With this configuration, the supercapacitor is discharged only when the LTC3108 DC-DC converter is not harvesting energy ($V_{out} < 4.8$ V, if we considered the voltage drop of the Schottky diodes as $V_D \approx 200$ mV). The LTC3108 has a quiescent current that can reach up to 9 μ A, so diodes D_1, D_2 are necessary to prevent the internal circuits of the LTC3108 from discharging capacitors C_{out} and C_{Cstore} when the microgenerator is not operating.

The output voltage from the ORed connection is sent to two voltage regulators: IC_1 , a 3.0-V output low drop-out voltage regulator (LDO) TPS70930 (from Texas Instruments), which has a very low quiescent current, typically 1 μ A; and IC_2 , a 5.0-V output high-efficiency charge pump DC-DC converter (TPS60130, from Texas Instruments), which can operate from input voltages as low as 2.7 V and provides a $5.0 \pm 4\%$ -V output voltage.

The 3.0-V from the LDO is used to power the MSP430F6736 microcontroller (from Texas Instruments). The 5.0-V output from the TPS60130 is sent to two LM2662 Positive/Negative Charge Pumps (from Texas Instruments). The LM2662 is very versatile and provides an output that can either double or invert its input voltage. Therefore, in our circuit, the 5.0 V are doubled by IC_3 (generating a 10-V output) and inverted by IC_4 , generating a −5 V output.

To measure soil water content with high precision (usually a 1% resolution in θ_v is required [20]), it is necessary to apply well-controlled pulses of power to heat the transistor. Unfortunately, the output voltage of the LM2662 is not regulated, presents high ripple, and varies with the temperature and also with load current.

Thus, to obtain a well-known and stable voltage, we needed to send the 10-V output from IC_3 to an adjustable LDO, IC_5 , a TPS71501 (from Texas instruments), which has a power supply ripple rejection of 60 dB, a line regulation of 61 dB, a load regulation of 60 dB and, and output thermal coefficient $TC \approx 15 \text{ ppm}/^\circ\text{C}$. In our circuit, the TPS71501 was designed to furnish an 8.0-V regulated output voltage, by adjusting resistors R_1 and R_2 .

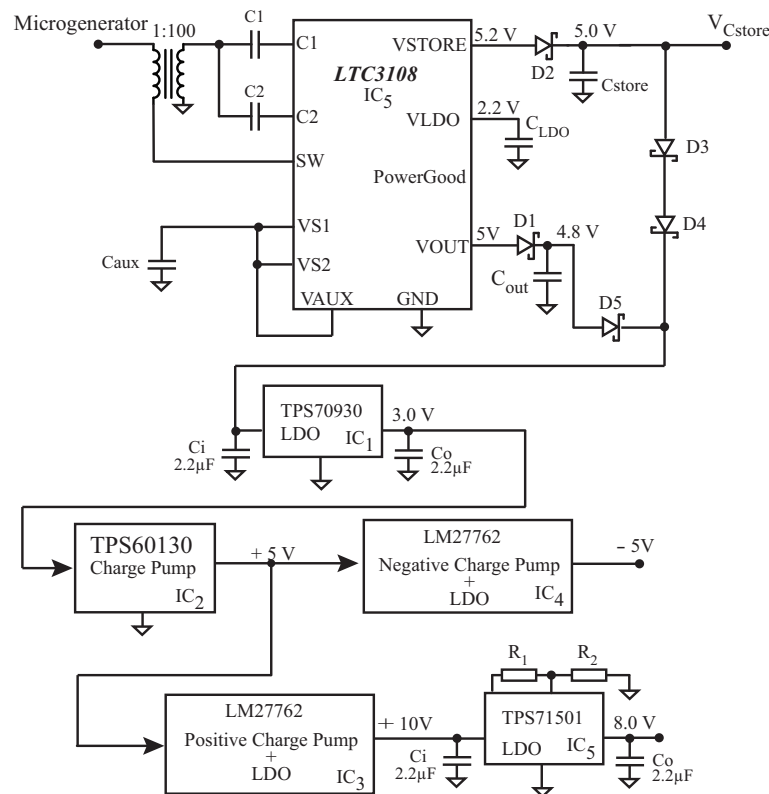


Figure 2. Basic diagram of the power management circuit. LDO, low drop-out voltage regulator.

3.2. Sensor Biasing and Heat Pulse Circuit

The simplified schematic of the bias and heat pulse circuit used to drive the sensor (an NPN transistor) is presented in Figure 3. The base is maintained at a fixed voltage, derived from a temperature-stable voltage reference $V_{REF1} = 1.25 \text{ V}$ (REF3312 from Texas Instruments).

The emitter is connected to a current source, which has its value switched between two values (100 μA and 10 mA), by the action of a single pole dual throw switch SW_1 (SPDT) on a resistor. The current source is defined by the voltage reference $V_{REF2} = 1.25 \text{ V}$ (also an REF3312 from Texas Instruments), op-amp A_1 (LTC6003, a rail-to-rail ultra-low supply current, low off-set and low-bias current op-amp from Analog Devices), an NMOS transistor M_1 (VN2222), and resistors R_1, R_2 . Transistor M_1 is inside the negative feedback loop, and op-amp A_1 forces $V_S = V_{REF2}$. Therefore, the drain current in M_1 , which is equal to the emitter current of Q_1 , is given by:

$$I_{E1} = \frac{V_{REF2}}{R_{eq}} \quad (5)$$

where $R_{eq} = R_1$ when SW_1 is opened and $R_{eq} = R_1 // R_2$ when SW_1 is closed. The values of $V_{REF2}, R_1,$ and R_2 are calculated to furnish the desired currents of 100 μA and 10 mA.

During the heat pulse, both the voltage V_{CB} and the emitter current are kept constant, but the variation of temperature in the transistor causes some changes in the value of V_{CE} . Since during the heat pulse, the maximum temperature variation in an SHPP is usually in the order of 5°C , the variation of V_{BE} with temperature (which changes the value of V_{CE}) will be only in the order of 9 mV (only 1.2 ppm

of variation in V_{CE} . Furthermore, the typical variation of β_F with temperature (which changes the base current) is only $0.35\%/^{\circ}\text{C}$ [15], so we can assume that the power dissipated in the transistor is constant during the heat pulse.

To measure the V_{BE} of the sensor transistor, two unity gain amplifiers A_3, A_4 , implemented with an LTC6004 (a dual version of the LTC6003 op-amp), are connected to the emitter and base terminals of the sensor. The outputs of the op-amps are sent to a differential analogue-to-digital (A/D) converter available in the MSP430F6736 microcontroller (from Texas Instruments), which operates with a supply current of only $1.25\ \mu\text{A}$ in low-power mode, with the real-time clock (RTC) running. Although the MSP430F6736 A/D converter has 24 bits, we used only 16 bits (15 bits plus one sign bit), which was enough to measure V_{BE} with a $\approx 36.6\text{-}\mu\text{V}$ resolution.

In this initial phase of measurement (which lasted only 50 ms), the measured value of V_{BE} was used to calculate the equilibrium temperature between the sensor and the soil before the heat pulse was applied. Measuring the soil's temperature is very important because a calibration curve (deviation of the measured value as a function of the soil temperature) has to be obtained experimentally, before using the sensor in the soil [21]. The V_{CB} voltage in the transistor was kept constant ($V_{CB} = 6.75\ \text{V}$), and since the transistor's emitter current during this measurement phase was $100\ \mu\text{A}$, the power applied to the transistor was very low ($P = I_E V_{CE} \approx 730\ \mu\text{W}$); thus, the sensor's temperature was practically not affected.

During the heat pulse phase, which in our prototype lasted 10 s, the collector voltage was kept unchanged ($V_C = 8\ \text{V}$, so $V_{CE} \approx 7.45\ \text{V}$), while the current was increased from $100\ \mu\text{A}$ – $10\ \text{mA}$ (with switch S_{W1}), generating a heat pulse with approximately $E = 0.745\ \text{J}$ ($74.5\ \text{mW}$ during 10 s). Switch S_{W1} is controlled by the I/O pins of the microcontroller, but since it is biased with GND and $-5\ \text{V}$, a level shift circuit is required to actuate in the digital inputs of S_{W1} .

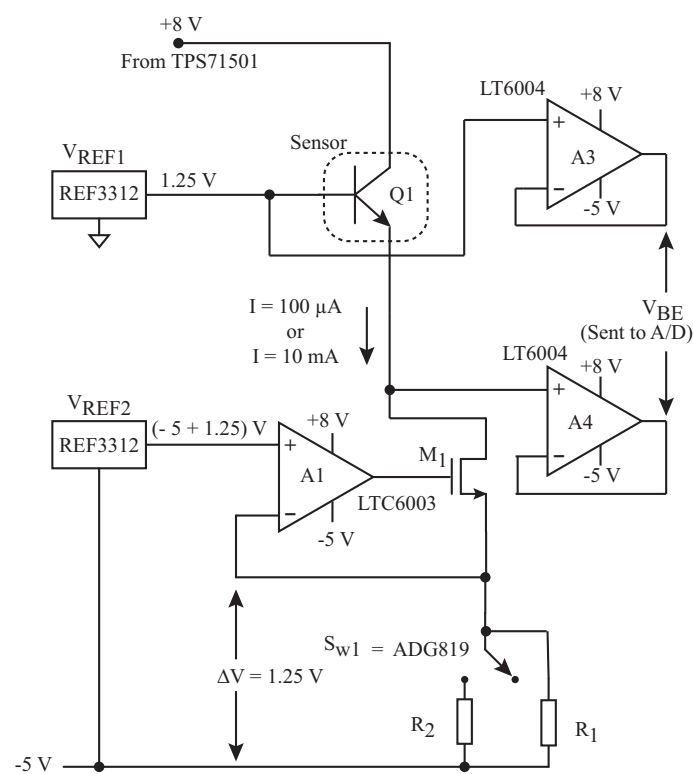


Figure 3. Basic diagram of the sensor's bias and heat pulse circuit.

In the built prototype, we decided to store the measured values of V_{BE} in a secure digital card (SD card), so we could analyze the data and plot the curves of V_{BE} as a function of the time, to verify if the sensor was working properly. The A/D converter was programmed to make, for every second,

ten measurements (one at each 10 ms). Next, for these ten measured points, the microcontroller calculated the mean of the first five points (M_i) and the mean of the last five points (M_f). Finally, the mean $(M_i + M_f)/2$ was calculated and written to the SD card.

Except for the period when the heat pulse was being applied, the current consumption of the conditioning circuit was very low (approximately $2.5 \mu\text{A}$) because, except for the voltage regulator IC_1 and the microcontroller, the rest of the circuit was in shut-down mode. Since the current during the heat pulse was 10 mA during 10 s, the average current consumption of the complete circuit was only $3.7 \mu\text{A}$, and laboratory tests showed that even if the harvesting system is not operating, a 2-F supercapacitor charged with 5 V can keep the circuits working for more than eleven days.

4. Materials and Methods

Sensor Construction

A half-hole was drilled in the center of a commercial porous ceramic block (from Hidrosense), and a 2N2222 transistor with a metal can package was inserted in the half-hole. The empty volume inside the hole, which is not occupied by the transistor, was filled with a 20.7-W/m K high thermal conductivity epoxy, Epotherm 130, from Transene, Inc. A sectional view and a photograph of the fabricated sensor are presented in Figure 4.

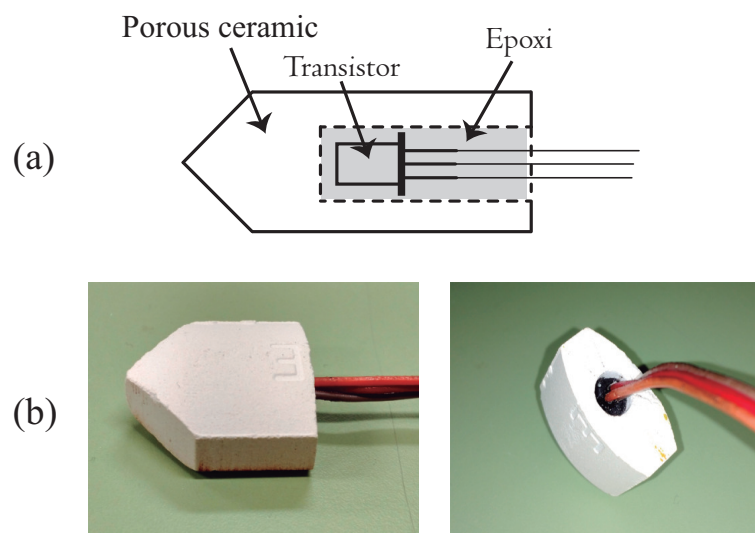


Figure 4. (a) Sectional view; (b) photograph of the fabricated sensors.

5. Test Protocol

5.1. Measurement with the Sensor Not Inserted in the Soil

The operation of soil water matric potential sensors based on the porous block depends basically on the characteristics of the porous ceramics. Thus, the first test performed was an evaluation of the sensor's response for different values of the volumetric water content in the porous block, by measuring the V_{BE} of the sensor as a function of the time.

To avoid the presence of entrapped air in the pores, the sensor was soaked for twelve hours in water (at atmospheric pressure), followed by an additional one hour under a pressure of approximately 70 kPa, to guarantee a complete saturation of the ceramic [12]. Based on the observed weight change from dry to saturated, the saturated volumetric water content of the porous ceramic was calculated as $\theta_v = 46.4\%$.

Next, the saturated sensor was placed on a scale (with a 0.1-g resolution) and left in an ambient condition with controlled temperature ($25 \pm 2 \text{ }^\circ\text{C}$). During the evaporation process, for different values

of θ_v , heat pulses were applied, and measurements of V_{BE} as a function of the time were taken during each pulse.

The volumetric water content θ_v of the porous ceramic is defined as the weight of water absorbed into the soil divided by the weight of the porous ceramic. The value of θ_v is commonly presented in %. In this prototype, the measured values of V_{BE} were not converted to temperature inside the microcontroller. The values of V_{BE} recorded in the SD card were read in a PC, where they were converted to temperature using a spreadsheet that calculated Equations (2) and (3).

It is worth noticing that for the operation of the sensor in the field, it is not necessary to calculate the values of temperature. If we measure the initial and final V_{BEs} of the transistor, using Equation (3), we can write:

$$V_{BE}(T_0) = \left(V_{g0} + \eta \frac{kT_r}{q} \right) - \lambda T_0 \quad (6)$$

and

$$V_{BE}(T_f) = \left(V_{g0} + \eta \frac{kT_r}{q} \right) - \lambda T_f \quad (7)$$

Thus, subtracting Equation (7) from Equation (6), we obtain:

$$V_{BE}(T_0) - V_{BE}(T_f) = \lambda(T_f - T_0) \quad (8)$$

Therefore, the difference $(T_f - T_0)$ is proportional to $\Delta V_{BE} = V_{BE}(T_0) - V_{BE}(T_f)$, and during the calibration in the laboratory, the values of θ_v should be calibrated as a function of ΔV_{BE} . This value can be easily calculated inside the microcontroller and used by the automatic irrigation system.

The values of the calculated temperatures (as well as the temperature difference between $t_0 = 1$ s and $t_f = 10$ s, as a function of time) are simultaneously plotted in Figure 5, for values of θ_v between 6% and 46.4%. In Figure 6, we present a plot of the calculated values of ΔT (measured at $t = 10$ s) as a function of θ_v .

It is important to observe that, for $\theta_v = 40\%$, the value of ΔT in this sensor (with an energy heat pulse $E = 0.745$ J) was $\Delta T \approx 3.1$ °C, while in [13], where the transistor was in direct contact with the soil and the energy heat pulse was 100% higher, the value of ΔT was $\Delta T = 4.5$ °C, which is only 45% higher.

However, this does not imply that the sensor with the porous block is more energy efficient. This difference found in ΔT occurred simply because we had two different mediums serving as a heat sink for the transistor: the porous ceramic saturated with water and the soil saturated with water. Considering that the ratio of the thermal resistivity between a soil with a high organic content and a quartz sand soil can be as high as 3:1 [22], it is clear that what happens here is that, when saturated with water, the ceramic had a higher thermal resistance than the soil used in the experiment conducted in [13].

Although the measured response of ΔT as a function of water content in the ceramic was clearly non-linear (see Figure 6), we can evaluate the sensor's worst case sensitivity (that occurred in the region $25\% \leq \theta_v \leq 46.4\%$) as $S = 0.023$ °C/%. Since the 15-bit A/D converter used can read the V_{BE} of the transistor with a 36.6- μ V resolution, which corresponds to a resolution of approximately 0.020 °C, the water content in the ceramic can be read in increments of approximately 0.87%.

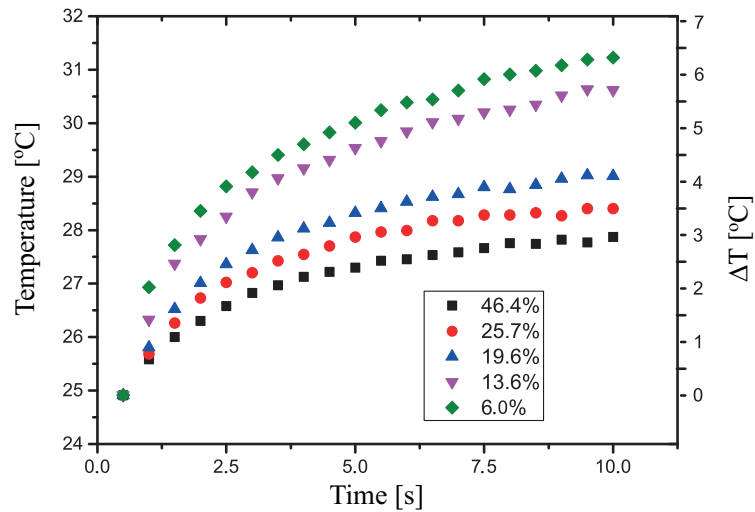


Figure 5. Plot of the measured temperature T and the temperature difference ΔT , as a function of time, for several values of θ_v .

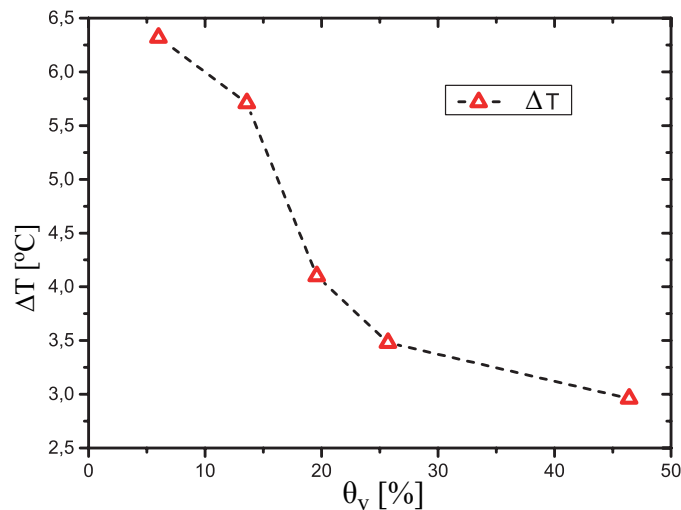


Figure 6. Plot of ΔT as a function of θ_v , measured at $t = 10$ s (calculated from the measured values of V_{BE}).

5.2. Measurement with the Sensor Inserted in the Soil

Next, the sensor was inserted in a clayey red latosol with the following composition: 0.65 kg kg^{-1} clay, 0.21 kg kg^{-1} silt, and 0.14 kg kg^{-1} sand; and a second test was carried out to measure its output as a function of small differences in matric potentials. When the water retention curve of this soil was measured for small matric potentials between 1 kPa and 35 kPa, a practically linear behavior was observed [23].

An inverted Richards chamber [24] was used, and the soil was submitted to pressures between 1 kPa and 35 kPa, to see how the sensor behaved for small changes in the matric potential in the soil. A photograph of the inverted Richards chamber and the equivalent schematic drawing are shown in Figure 7.

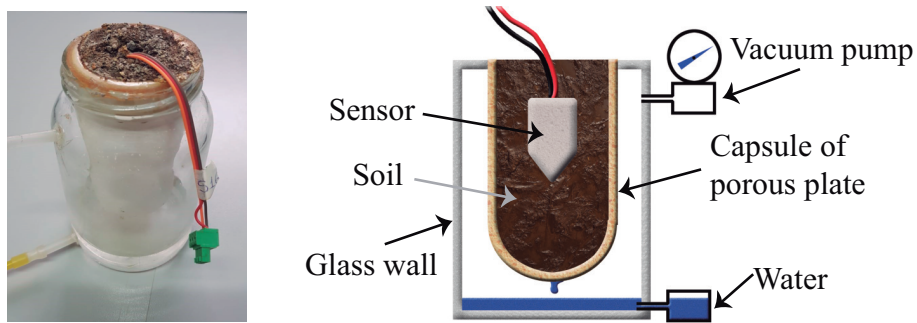


Figure 7. Photograph and schematic diagram of the inverted Richards chamber.

A minimum time interval of 12 h between measurements was used, to guarantee that an equilibrium between the water in the porous sensor and the in soil was reached before each measurement. From the results presented in Figure 8, we observed a practically linear behavior as a function of the matric potential. From Figure 8, we can see that, in this small region, the sensor presented a sensitivity of approximately $S = 0.015 \text{ }^\circ\text{C/kPa}$.

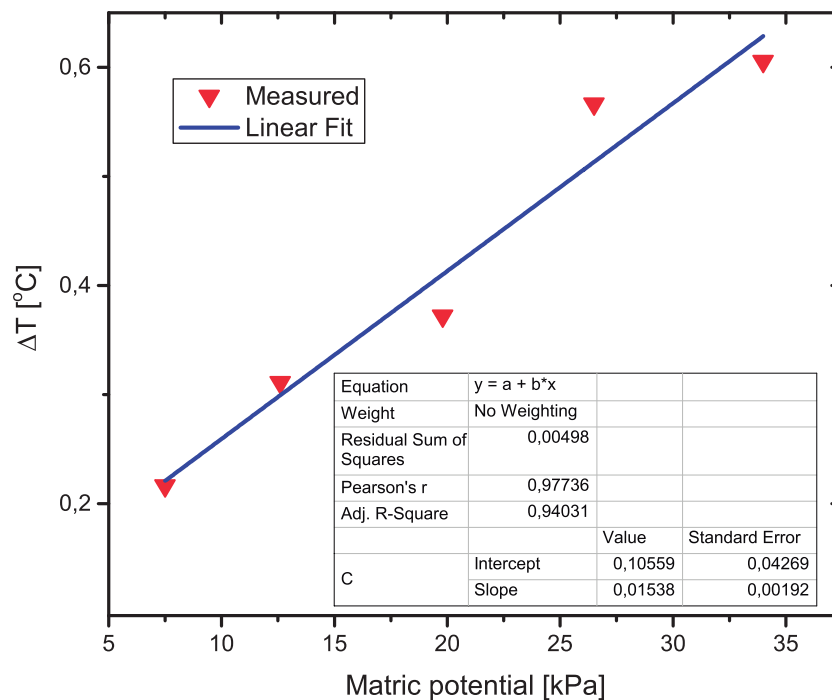


Figure 8. Plot of ΔT as a function of the soil matric potential, measured at $t = 10 \text{ s}$ (calculated from the measured values of V_{BE}).

5.3. Repeatability Tests

To evaluate the repeatability of the sensor, two sensors were measured with the porous ceramic in two different conditions: saturated and oven dried. The sensor was put inside a closed box, with thermal insulation and temperature control, and the temperature was maintained at $21 \pm 0.03 \text{ }^\circ\text{C}$. For each water content of the sensor, the V_{BEs} of each sensor was measured five times, with an interval of 20 min between measurements, to guarantee that, even after receiving the heat pulse, the sensor was at the desired initial temperature.

Table 1 shows the results of the repeatability test for V_{BE} measurements, taken at $t_f = 10 \text{ s}$, in two sensors (S_1 and S_2). The highest value of the standard deviation was found to be 0.36 mV, which is three orders of magnitude smaller than the mean value 866.76 mV. This highest standard deviation was

measured when the ceramic of sensor S_2 was saturated. These small variations can be explained by the slight uneven redistribution of the water inside the ceramic that may occur between each measurement, after the heat pulses.

Table 1. Measured values of V_{BE} (mV) in two sensors (S_1 and S_2) with two different water content conditions: dry and saturated.

Sensor #	S_1	S_1	S_2	S_2
Condition	Saturated	Dry	Saturated	Dry
Meas. #1	865.49	859.45	866.68	859.08
Meas. #2	865.40	860.18	867.14	859.17
Meas. #3	864.89	859.86	867.09	859.22
Meas. #4	865.12	860.09	866.64	858.58
Meas. #5	864.89	860.05	866.27	858.76
Avg.	865.16	859.93	866.76	858.96
Std. Dev. (σ)	0.28	0.29	0.36	0.28

6. Conclusions

A soil water content sensor based on a single transistor encapsulated in a porous ceramic block was fabricated and tested in the laboratory. The sensor was tested with volumetric water contents in the ceramic in the range of $6\% < \theta_v < 46.4\%$. With the porous ceramic saturated ($\theta_v = 46.4\%$), the temperature difference measured was $\Delta T = 2.9^\circ\text{C}$. For a dry ceramic ($\theta_v = 6\%$), the value of the ΔT was 6.3°C . The sensor's sensitivity, calculated in the worst case condition (between $25\% \leq \theta_v \leq 46.4\%$) was $S = 0.023^\circ\text{C}/\%$. The 15-bit A/D converter used can read the V_{BE} of the transistor in steps of $36.6\ \mu\text{V}$, which corresponds to a temperature resolution of approximately 0.02°C , so θ_v can be read in increments of at least 0.87% .

When tested inserted in a red latosol, the sensor presented an almost linear behavior for small changes in the matric potential of the soil, between 1 kPa and 35 kPa. In this small region, the sensor presented a sensitivity of $S = 0.015^\circ\text{C}/\text{kPa}$. The sensor presented in this work is a great improvement over the previous work because it does not have the soil contact problem (as it is based on a porous block), and the addition of the porous block does not reduce the energy efficiency of the sensor. The novel ultra-low power circuit conditioning circuit developed was designed to be used powered by an energy-harvesting systems. When powered by a 2-F supercapacitor, the signal conditioning circuit operated continuously for eleven days, making one soil water content measurement per day.

Author Contributions: Conceptualization, P.C.-D.; formal analysis, P.C.-D.; investigation, J.A.S.D., P.C.-D., F.J.O.M. and L.F.C.D.; methodology, J.A.S.D., P.C.-D., F.J.O.M. and A.C.; software, F.J.O.M.; supervision, J.A.S.D. and A.C.; validation, J.A.S.D. and F.J.O.M.; writing, original draft, J.A.S.D. and A.C.; writing, review and editing, J.A.S.D. and A.C.

Funding: We thank Hidrosense Ltda for making the measurements of the sensor with the Richards chamber and for supplying the porous ceramic blocks used in the fabrication of the sensor.

Conflicts of Interest: The authors declare no conflict of interest. The funders had no role in the design of the study; in the collection, analyses, or interpretation of data; in the writing of the manuscript; nor in the decision to publish the results.

Abbreviations

The following abbreviations are used in this manuscript:

A/D	Analog-to-digital
BHPP	Button heat pulse probe
C_{store}	Value of the supercapacitor
DHPP	Dual heat pulse probe
E	Energy in the heat pulse
I_C	Collector current

k_s	Thermal conductivity of the soil
NMOS	N channel MOS transistor
Q_l	Heat input per unity length of the heater
RTC	Real-time clock
S	Sensitivity of the sensor
T	Temperature in °C
SHPP	Single heat pulse probe
t_0	Initial time of heat pulse
t_f	Final time of heat pulse
T_0	Initial temperature of the sensor
T_f	Final temperature of the sensor
V_{BE}	Base to emitter voltage
V_{g0}	Silicon bandgap at 0 K
V_{out}	Output voltage of the DC-DC converter
V_{REF}	Temperature-stable voltage reference
V_{CB}	Collector to base voltage
V_{CE}	Collector to emitter voltage
η	Constant dependent on the fabrication process of bipolar transistors
λ	Linear part of the thermal coefficient of V_{BE}
ΔT	Temperature difference between the hot and cold side of a TEG
β_F	Current gain in the common emitter
θ_v	Soil water content
η	Constant dependent on the fabrication process of bipolar transistors
λ	Linear part of the thermal coefficient of V_{BE}
Δt	Duration of the heat pulse

References

- Brase, T. *Precision Agriculture*; Thomson Delmar Learning: New York, NY, USA, 2006.
- Rivers, M.; Coles, N.; Zia, H.; Harris, N.R.; Yates, R. How Could Sensor Networks Help With Agricultural Water Management Issues? Optimizing Irrigation Scheduling Through Networked Soil-Moisture Sensors. In Proceedings of the IEEE Sensors Applications Symposium (SAS), Zadar, Croatia, 13–15 April 2015.
- Pelletier, M.G.; Scharz, R.C.; Holt, G.A.; Wanjura, J.D.; Green, T.R. Frequency Domain Probe Design for High Frequency Sensing of Soil Moisture. *Agriculture* **2016**, *4*, 60. [[CrossRef](#)]
- Hanson, B.R.; Peters, D.; Orloff, S. Effectiveness of tensiometers and electrical resistance sensors varies with soil conditions. *Calif. Agric.* **2000**, *54*, 47–50. [[CrossRef](#)]
- Kamai, T.; Kluitenberg, G.J.; Hopmans, J.W. Design and numerical analysis of a button heat pulse probe for soil water content measurement. *Vadose Zone J.* **2009**, *8*, 167–173. [[CrossRef](#)]
- França, M.; Morais, F.; Carvalhaes-Dias, P.; Duarte, L.; Siqueira Dias, J. A Multiprobe Heat Pulse Sensor for Soil Moisture Measurement Based on PCB Technology. *IEEE Trans. Instrum. Meas.* **2019**, *68*, 606–613. [[CrossRef](#)]
- Valente, A.; Morais, R.; Couto, C.; Correia, J.H. Modeling, simulation and testing of a silicon soil moisture sensor based on the dual-probe heat-pulse method. *Sens. Actuators A Phys.* **2004**, *115*, 434–439. [[CrossRef](#)]
- Li, M.; Si, B.C.; Hub, W.; Dyck, M. Single-Probe Heat Pulse Method for Soil Water Content Determination: Comparison of Methods. *Vadose Zone J.* **2016**, *7*. [[CrossRef](#)]
- Shiozawa, S.; Campbell, G. Soil thermal conductivity. *Remote Sens. Rev.* **1990**, *5*, 301–310. [[CrossRef](#)]
- Dias, P.C.; Cadavid, D.; Ortega, S.; Ruiz, A.; França, M.B.; Morais, F.J.; Ferreira, E.; Cabot, A. Autonomous soil moisture sensor based on nanostructured thermosensitive resistors powered by an integrated thermoelectric generator. *Sens. Actuators A Phys.* **2016**, *239*, 1–7. [[CrossRef](#)]
- Phene, C.J.; Hoffmna, G.J.; Rawlins, S. Measuring soil matric potential in situ by sensing heat dissipation within a porous body. *Soil Sci. Soc. Am. Proc.* **1971**, *35*, 27–33. [[CrossRef](#)]
- Costa, E.F.; Oliveira, N.E.; Morais, F.J.O.; Carvalhaes-Dias, P.; Duarte, L.; Cabot, A.; Siqueira Dias, J. A Self-Powered and Autonomous Fringing Field Capacitive Sensor Integrated into a Micro Sprinkler Spinner to Measure Soil Water Content. *Sensors* **2017**, *17*, 575. [[CrossRef](#)] [[PubMed](#)]

13. Dias, P.C.; Roque, W.; Ferreira, E.; Siqueira Dias, J.A. A high sensitivity single-probe heat pulse soil moisture sensor based on a single npn junction transistor. *Comput. Electron. Agric.* **2013**, *96*, 139–147. [[CrossRef](#)]
14. Dias, P.C.; Morais, F.J.M.; França, M.B.; Ferreira, E.C.; Cabot, A. Autonomous Multi-sensor System Powered by a Solar Thermoelectric Energy Harvester with Ultra-Low Power Management Circuit. *IEEE Trans. Instrum. Meas.* **2015**. [[CrossRef](#)]
15. Meijer, G. Integrated Circuits and Components for Bandgap References and Temperature Transducers. Ph.D. Thesis, TU Delft, Delft, The Netherlands, 1982.
16. Carvalhaes-Dias, P.; Guimaraes, H.L.; Siqueira Dias, J.A. High Precision PTAT current source based on the Meijer cell. *Int. J. Electron.* **2017**, *104*, 2099–2110. [[CrossRef](#)]
17. De Vries, D. Thermal properties of soil. In *Physics of Plant Environment*; van Wijk, W.R., Ed.; John Wiley and Sons: New York, NY, USA, 1963; pp. 210–234.
18. Kluitenberg, G.; Bristow, K.; Das, B. Error analysis of the heat pulse method for measuring soil heat capacity, diffusivity and conductivity. *Soil Sci. Soc. Am. J.* **1995**, *59*, 719–726. [[CrossRef](#)]
19. Carvalhaes-Dias, P.; Cabot, A.; Siqueira Dias, J. Evaluation of the Thermoelectric Energy Harvesting Potential at Different Latitudes Using Solar Flat Panels Systems with Buried Heat Sink. *Appl. Sci.* **2018**, *8*, 2641. [[CrossRef](#)]
20. Dias, P.; Morais, F.; França, M. Temperature-stable heat pulse driver circuit for low-voltage single supply soil moisture sensors based on junction transistors. *Electron. Lett.* **2016**, *52*, 208–210. [[CrossRef](#)]
21. Flint, A.; Campbell, G.; Ellet, K.; Calissendorff, C. Calibration and Temperature Correction of Heat Dissipation Matric Potential Sensors. *Soil Sci. Soc. Am. J.* **2002**, *66*, 1439–1445. [[CrossRef](#)]
22. Campbell, G. Thermal Resistivity of Porous Materials (Soils) Change with Changes in Density, Water Content, Temperature and Composition. In Proceedings of the Pittcon Conference & Expo 2016, Atlanta, GA, USA, 6–10 March 2016.
23. Benevenuto, P.; Passos, L.A.; Melo, L.B.; Silva, E.A.; Oliveira, G.C. Synthetic polymers on water retention and pore distribution in a clayey latosol. *Rev. Sci. Agrar.* **2016**, *17*, 24–30.
24. Richards, L.A. *Methods of Soil Analysis—Physical and Mineralogical Properties, Including Statistics of Measurements and Sampling*; The American Society of Agronomy: Madison, WI, USA, 1965.



© 2019 by the authors. Licensee MDPI, Basel, Switzerland. This article is an open access article distributed under the terms and conditions of the Creative Commons Attribution (CC BY) license (<http://creativecommons.org/licenses/by/4.0/>).